Glyndŵr University Research Online

Conference Presentation

Implementation of electrical rim driven fan technology to small unmanned aircraft

Bolam, R., and Vagapov, Y

Recommended citation:

Bolam, R., and Vagapov, Y (2017) 'Implementation of electrical rim driven fan technology to small unmanned aircraft. In: Proc. 7th IEEE Int. Conference on Internet Technologies and Applications ITA-17', Wrexham, UK, 12-15 September 2017, pp 35-40. doi: 10.1109/ITECHA.2017.8101907

Implementation of Electrical Rim Driven Fan Technology to Small Unmanned Aircraft

Robert Cameron Bolam, Yuriy Vagapov
School of Applied Science, Computing and Engineering
Glyndwr University
Wrexham, LL11 2AW, UK

Abstract—**Aircraft propeller performance is significantly reduced when tip speeds become sonic causing the maximum attainable airspeed of the vehicle to be limited by the propeller diameter. There are also performance losses attributable to miniature Unmanned Aerial Vehicles as the propeller to hub diameter ratio is reduced. The research conducted indicated that re-arranging a Brushless DC Motor and propeller configuration, so that it becomes rim-driven rather than hub-driven, would provide some performance and operational advantages and could inspire the design of novel high-speed Unmanned Aerial Vehicle configurations powered by hub-less, multi-stage contra-rotating electrical fan-compressors. This investigation involved analysis, design and testing a prototype, low cost, concept demonstrator Rim Driven Fan device in order to assess the feasibility of applying this technology to Small Unmanned Aircraft. It was demonstrated that Rim Driven Fan technology could be successfully applied to lift and propel a Small Unmanned Aircraft. However, the performance testing of the Rim Driven Fan demonstrated that in its prototype configuration it would not be as efficient as a conventional Brushless DC motor and propeller.**

Keywords—rim driven fan; small unmanned aircraft; unmanned air vehicles; drone; brushless dc motors; hub-less fan

I. INTRODUCTION

Small Unmanned Aircraft (SUAs), which are more commonly referred to as "Drones", are becoming increasingly popular in our society and are used in a wide range of commercial and recreational applications [1]. The vast majority of these aircraft are electrically powered and use Lithium Polymer (LiPo) batteries for on-board energy storage and Brushless DC (BLDC) motors to drive conventional two or three bladed propellers for propulsion. Many recreational users are keen to home-build their own drones and this has resulted in a healthy market for an extensive range of inter-compatible drone related components [2].

The conventional BLDC motor with a two or three bladed hub-driven propeller combination is very well suited to both multi-rotor and fixed wing aircraft applications (Fig. 1). However, it can also be restrictive to the operational performance of SUAs, as excessive propeller tip speeds can limit their performance and hence the maximum achievable airspeed attainable by an aircraft. Additionally, hub mounted motors can reduce thrust, especially if located in the prop-wash [3].

Rim driven devices are not a new concept. Indeed, a waterwheel is a rim driven device. The concept of a tip or rim driven propeller (RDP) or fan (RDF) is also well established. As far back as 1957 a mechanically rim driven ships propeller was proposed [4]. Since then, the implementation of electrical rim drives has become popular in marine applications and now rim driven propeller RDP devices for surface and submarine vessels are currently commercially available [5].

RDFs have also been considered in aerospace applications; In 1961, funded by a USA governmental contract the Ryan Aircraft Corporation developed the XV-5A pneumatically powered rim-driven "lift-fan" aircraft and more recently a team of engineers from the NASA Glenn Research Center [6] have studied a conceptual design of a 32 inch diameter levitated ducted fan intended for aircraft propulsion.

II. PROTOTYPE REQUIREMENTS

In order to provide guidance for the design and development of a prototype RDF device, a project specification was formulated. This defined the following essential and desirable features:

A. Essential Features

- Low project cost;
- Low lead time;
- Able to interface with existing off-the shelf low cost components such as: Flight Controller, Electronic Speed Controller (ESC) and LiPo battery technology;
- Possible to be made and tested within a typical Technical College Workshop environment. e.g. 3D printer with 150mm maximum component diameter capability;
- That it functions effectively and demonstrates the feasibility of a rim driven fan device being suitable for a small UAV application.

B. Desireable Features

- Allows Pulse Width Modulation (PWM) thrust control;
- Is an efficient device;
- Is capable of rotating up to high speeds e.g. in excess 5000 rpm;
- Has low vibration;
- Exhibits smooth and responsive speed control;

- Is able to lift its own weight (lift to weight ratio of 1 or more);
- Is simple in design (e.g. no Hall Effect feedback sensors etc.);
- Is self-starting;
- Is safe to operate;
- Allows contra-rotational fan installations to be easily achieved;
- Exhibits the potential to be adaptable for vectored thrust applications;
- Has the potential to allow high speed electrical flight to be achieved (increased fan pressure ratio);
- Offers the potential for miniaturisation and hub-less fan development.

Fig. 1. SUA with shrouded hub driven fans

III. ANALYSIS

Initial estimates of lift and power requirements were established using the following standard engineering equations.

A. Target Mass Value

An initial estimate of the prototype RDF device's target weight was required. To do this a reference weight value of a comparable conventional out-runner motor and propeller combination was used. The equipment selected for this purpose was the BLDC motor AX-2810Q KV 750 fitted with an 11" Gemfan propeller. The mass of this combination was measured at 89 grams.

It was anticipated that the prototype RDF unit would be heavier than an equivalent conventional out-runner owing to the additional material required for the motor housing and bearing support so the measured value was doubled and rounded up to give a target mass value of 180g (0.18 kg).

B. Energy Required to Achieve a Lift to Weight Ratio of 1

A lift to drag ratio of 1 means that the RDF unit should be able to create enough lift to support its own weight. Therefore, the energy required to maintain 9.81 m/s velocity to overcome the acceleration due to gravity:

$$E = \frac{1}{2}mv^2 = 0.5 \times 0.18 \times 9.81^2 = 8.66 \,\text{J} \tag{1}$$

where E is the energy [J], m is the target mass [kg], v is the required velocity [m/s].

C. Power Required to Achieve a Lift to Weight Ratio of 1

To overcome gravity 8.66 J of work is required to be done by the RDF on accelerating air in the way of thrust every second. Therefore, the power required for this action is 8.66 W. A value of 50% efficiency us assumed for the fan and a value of 90% efficiency is assumed for both the motor and ESC Taking into account a design margin, the required power became:

$$P_R = \frac{aP}{\eta_F \eta_M \eta_{ESC}} = \frac{2.5 \times 8.66}{0.5 \times 0.9 \times 0.9} = 53.46 \,\text{W} \tag{2}$$

where P_R is the required power [W], a is the factor of 2.5 was applied to this value as a design margin, η_F is the efficiency of the fan, η_M is the efficiency of the motor, η_{ESC} is the efficiency of ESC.

D. Torque Required to Achieve a Lift to Weight Ratio of 1

A nominal operational speed value of $n = 5000$ rpm is initially selected for the RDF in order to estimate the required torque:

$$T = \frac{P_R \times 60}{2\pi n} = \frac{53.46 \times 60}{2\pi \times 5000} = 0.102 \,\text{Nm} \tag{3}$$

where T is the required torque [Nm], n is the operational speed [rpm].

E. Tangential Force Required at the Rim of the RDF

Assuming the outer RDF housing diameter could not exceed 150mm a rotor diameter of 124mm was estimated. This provided a radius arm value of 62mm from the centre of the rotor to the rim. Therefore, the required tangential force on the rim became:

$$F = \frac{T}{R} = \frac{0.102}{0.062} = 1.65 \,\text{N} \tag{4}$$

where F is the required force [N], R is the proposed radius [m].

F. ESC Current Rating

Checking the current rating required for the ESC to drive the RDF unit from a 10V DC supply:

$$I = \frac{P_R}{V} = \frac{53.46}{10} = 5.346 \,\text{A} \tag{5}$$

where I is the ESC current [A], V is the power supply voltage [V].

This current value is the maximum expected and would reduce if a 3S (11.1V) or 4S (14.8V) battery is configured to supply the ESC.

IV. ELECTRO-MAGNETIC CIRCUIT CALCULATIONS

A. Tangential Rotor Force

The electro-magnetic flux, generated by the conductors, in the air gap between the stator and rotor determines the magnitude of the tangential force exerted on the rim of the rotor. The following equation is used to calculate the tangential force:

$$F = BIl \qquad (6)$$

where B is the magnetic flux density [T], l is the length of the conductor [m].

Good machine design practice maintains the maximum magnetic flux density in the iron parts of the electro-magnetic circuit to 1.6 T. Above this value the iron starts to saturate and the magnetisation process becomes inefficient. Also, the DC power supply unit available to run the prototype units has a maximum current rating of 2.5 A, so a slightly lower operational value of 2.0 A was chosen for the prototype circuit design purposes.

Assuming the required tangential force of 1.65 N will be produced by one of the three sets of windings which each have four coils connected in parallel, then:

$$I_C = \frac{I}{k} = \frac{2}{4} = 0.5\text{A} \qquad (7)$$

where I_C is the current per coil [A], k is the number of coils connected in parallel ($k = 4$).

Therefore, the length of the conductor required is:

$$l = \frac{F}{BI} = \frac{1.65}{1.6 \times 2} = 0.516\text{m} \qquad (8)$$

The mean diameter of each coil is 5mm therefore the number of turns per coil is:

$$N = \frac{l}{\pi d} = \frac{0.516}{\pi \times 0.005} \approx 33\text{Turns} \qquad (9)$$

where N is the number of turns per coil [Turns], d is the mean diameter of reach coil [m].

The above value of turns per coil has been calculated assuming that the flux density in the air-gap is 1.6 T. However, this is determined by the total flux in the circuit which is iteratively dependent on the magnetising force based on the number of turns and current flowing in the coils.

B. Total Magnetic Flux

The value of flux density B in the above equation is that generated by the electro-magnetic circuit. This can be calculated once the total flux Φ in the circuit is known. However, determining the magnetic flux distribution in an electro-magnetic device can be very difficult to achieve with any degree of accuracy. Especially if the circuit being analysed is of a non-conventional arrangement such as the RDF under consideration. The major factors affecting the pattern of flux distribution are: the available magneto-motive force (m.m.f.) of the coil; the total reluctance of the circuit and the effects of any

magnetic leakage and fringing. The following equation was used to calculate the total flux:

$$\Phi = \frac{F_M}{\mathfrak{R}} = \frac{NI_C}{\mathfrak{R}} \qquad (10)$$

where Φ is the total flux [Wb], F_M is the mmf of the coil [A×Turns]; $\mathfrak{R}$ is the total reluctance [Wb/A×Turns].

The total reluctance of the circuit was established from the physical geometry of the magnetic circuit path and the permeability of the various materials in the circuit. The following equation was used to calculate the total reluctance:

$$\mathfrak{R} = \sum_{i=1}^{m} \frac{l_i}{\mu_0 \mu_i A_i} \qquad (11)$$

where $\mu_0 = 4\pi \times 10^{-7}$ H/m magnetic constant, μ_i is the relative permeability, A_i is the cross-sectional area [m²], l_i is the mean length [m].

The analysis of the electromagnetic circuit of the RDF device was carried out using the following two methods:

- Initial estimates and sizing calculations using standard textbook equations;
- Empirical data used for confirmation and validation of the above methodology.

V. PROTOTYPE RDF DESIGN

A. Motor Design, Winding Patterns and Pole Layouts

The design of the electromagnetic circuit of a motor is critical to its success. The layout of the stator windings not only effects m.m.f. produced but also whether the stator windings will be balanced. This ensures that all three phases produce the same level of back e.m.f. (BEMF) and that they are all out of phase by 120°. The selection and arrangement of the permanent magnets effect the flux density in the airgap and the start-up torque characteristics of the motor [7]. Fortunately, various papers and computer software packages such as MotorSolve [8] have been produced to assist in this process.

Very little guidance literature could be found relating to multi-pole stator/slot (winding) combinations. Radial flux architectures appear more widely used than axial machines and the most common radial flux arrangement used on SUAs such as quadcopters are 14 magnetic poles and 12 slots (windings).

Hendershot and Miller in [9] on BLDC motor phase, pole and slot configurations provide tables of recommended stator slot/rotor pole combinations for 3 phase BLDC motors. Twelve slots per winding was commonly listed alongside 4, 8 and 16 magnetic pole configurations. However, it was decided 12 clockwise windings, 8 magnetic poles and a 1.5 slot to pole ratio would be an optimum configuration. This was therefore selected for the prototype RDF device (Fig. 2).

In line with the common practice for virtually all small BLDC motors, the "wye" (star) connection pattern was selected for the windings. Connecting the circuit in a wye pattern means that two of the windings will always be in series and share the line voltages between their respective phases.

This means that the supply voltage to the windings is increased by a factor of 1.73 or √3, than if they had been connected in the delta pattern [10].
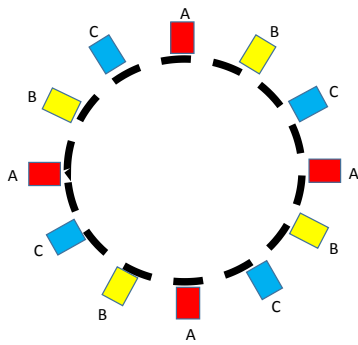

Fig. 2. Selected RDF stator winding pattern.

Theoretically the RDF device should be able to operate with the windings configured in parallel or series. The choice of which is a trade-off between:

- Parallel windings; these offer the potential for less impedance in the circuit and permit a greater current to flow generating more magneto motive force (m.m.f.).
- Series windings with higher circuit impedance, less m.m.f. but increased inductance and the likelihood of a strong BEMF signal for ESC.

It was decided that both parallel and series configurations would be trialed during the testing of the RDF unit.

The ESC converts the direct current (DC) battery supply to an alternating current (AC) to correctly energise the BLDC stator windings and generate the rotating magnetic field. The process of ensuring that the current is always flowing in the correct direction in the stator windings is known as "commutation" and this controls the changing polarity of the magnetic field. The permanent magnet (PM) rotor "locks" on to the stator field and then rotates at the same speed, thus ESCs can also be known as Synchronous Motor Drives or Electronically-Commutated Motor (ECM) drives.

The AC drive signal is 3-phase and is generated by a 3-phase inverter which comprises of solid state switching devices known as MOSFETs arranged in a transistor bridge as shown in Fig. 3.

To ensure stable "closed loop" speed control the ESC hardware also incorporates a microcontroller which runs a pre-programmed software algorithm or Firmware. On multi-rotor UAVs, it is the ESC commands alone that stabilise the aircraft by constantly varying the BLDC motor speeds in accordance with the Firmware control logic. The inputs to the ESC are derived from the Flight Controller (FC) which contains the IMU (Inertial Measurement Unit) and the GPS (Global Positioning System). Additional input sensor data may also be received from 3d-Magnetometer/compass, ultrasonic sensors, pressure or temperature sensors etc. [11].

Normally the speed of the motors used in SUAs is manually adjusted using the throttle control on the transmitter unit. However, for the purpose of testing the RDF device, a servo adjuster unit was implemented instead.
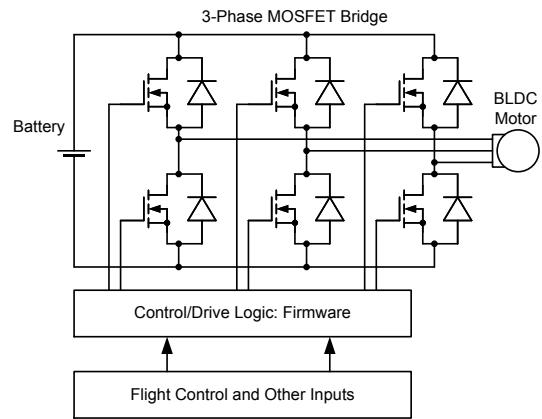

Fig. 3. A structure of BLDC motor control.

The motor speed is determined by the speed of the rotating magnetic field, which is known as the synchronous speed n_s. This is directly proportional to the frequency (f) of the 3-phase electrical supply and inversely proportional to the number of stator poles (p) as defined by the following equation:

$$n_s = \frac{120f}{p} = \frac{120 \times 500}{12} = 5000 \text{rpm} \tag{12}$$

Positional or speed feedback from the motors is also required to stabilise a BLDC motor system. This is normally provided by Hall Effect Sensors or encoder devices which are integrated within each motor. However, on most small UAVs, the ESC achieves this simply by monitoring the back e.m.f. waveforms from each energised winding in the 3-phase motor cycle.

Therefore, it was important to make sure that the RDF device also produced a similar or adequate back e.m.f. signal that registers with the ESC. This was done by designing the coils to match or exceed the inductance values of existing BLDC motor devices.

B. Fan Design

The thrust developed by a propeller or fan is a product of the mass-flow of air passing through the fan and its associated increase in velocity.

$$Thrust = M(V_2 - V_1) \tag{13}$$

where M is the mass-flow [kg/s]; V is the velocity [m/s]

It follows that an equivalent amount of thrust can be obtained by either accelerating a large mass of air slowly or a smaller mass of air more quickly. The former method is more efficient than the latter as it involves a low pressure rise across the fan or propeller and therefore minimises the associated heating and turbulence losses. Thus, "large" propellers are efficient but limited to low speed flight, whereas "smaller" fans are suitable for higher flight speeds and compact propulsion unit designs.

The full analyses required to determine the most suitable fan device for an RDF was deemed beyond the scope of this feasibility study. However, a semi-empirical fan analysis and design process was adopted, in order to obtain an aerodynamic

fan shape that would be capable of sustaining an adequate pressure rise required to fulfil the following desirable (target) specification requirement: **able to lift its own weight** (lift to weight ratio equal or greater than 1)

The analysis involved the CFD modelling of candidate fan blade configurations derived from fan performance charts [12] until a suitable aerodynamic shape and number of fan blades was established. A rimless prototype fan was then constructed and installed on a conventional out-runner motor and tested for lifting performance under a range of speeds and powers (Fig. 4).
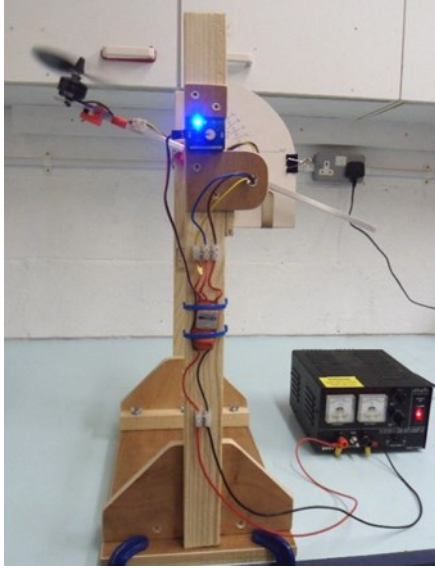

Fig. 4. The conventional BLDC motor and 4 bladed fan performance testing.

VI. PROTOTYPE RDF TEST RESULTS

The performance test results indicated that the RDF configuration was capable of achieving the "target value" Lift to Weight ratio of 1 (Fig. 5, Table I, Table II), although to do this the fan had to rotate at a much higher speed than the conventional BLDC i.e. 7000 rpm compared to 5500 rpm. It was interesting to note that the overall thrust efficiencies of both configurations remained comparable over the wide range of speeds tested. Additional maximum rotational speed tests, conducted under minimum thrust conditions, recorded speeds in excess of 10,000 RPM (Fig. 6).

TABLE I. CONVENTIONAL BLDC WITH HYBRID 4 BLADED FAN

Speed (rpm)	Input Voltage (V)	Input Power (W)	Lift/Weight Ratio	Thrust Efficiency
3097	11.5	5.75	0.26	41%
4680	11.5	13.8	0.69	45%
5500	11.5	21.3	1	42%

TABLE II. RDF CONFIGURED BLDC WITH HYBRID 4 BLADED FAN

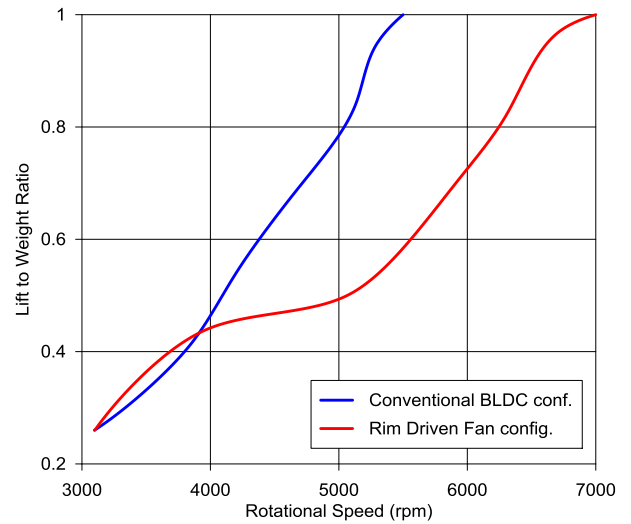| Speed (rpm)	Input Voltage (V)	Input Power (W)	Lift/Weight Ratio	Thrust Efficiency
3100	11.5	5.75	0.26	43%
5945	11.5	25.3	0.71	42%
>7000	14.8	>44	1	33%

Fig. 5. Performance comparison of BLDC and RDF motor technology.

Fig. 6. Prototype RDF unit running at speeds in excess of 10,000 rpm.

VII. RDF CONFIGURED FOR A HIGH SPEED FLIGHT

High speed flight involves accelerating the aircraft to a high speed relative to the ambient air and then maintaining enough thrust to overcome the drag incurred at this speed. In order to accelerate the air, the fan must impart energy to it, and thus increase its total pressure. The ratio of the fan outlet pressure to its inlet pressure is termed the Fan Pressure Ratio (FPR) and this is critical to determining the maximum speed that an aircraft may attain. Fan Pressure Ratios of 1.65 are normal values achieved with modern turbo-fan engines, which are capable of propelling aircraft to speeds in the region of Mach 0.8 [13].

The RDF design concept allows the arrangement of multiple fan rotors in tandem (Fig. 7). In addition, their combined efficiency may be improved when contra-rotating [3]. If each rotor installation is considered to be similar to an axial flow compressor stage, which typically has a pressure ratio (PR_{stage}) between 1.1 and 1.2 (say 1.15), then the total number of rotors required can be easily determined using the following equation:

$$\ln N_S = \frac{PR_{total}}{PR_{stage}} = \frac{1.65}{1.15} = 1.435 \qquad (14)$$

where: N_S is the number of rotor stages.

Therefore

$$N_S = e^{1.435} = 4.2 \approx 4 \qquad (15)$$

This simple calculation illustrates that the RDF concept has the potential to allow a UAV to achieve high speed subsonic flight with, for example, four well designed fan rotors arranged in tandem. Of course, much more detailed research and analysis would be required before confirmation of this basic *PR* assumption could be made.
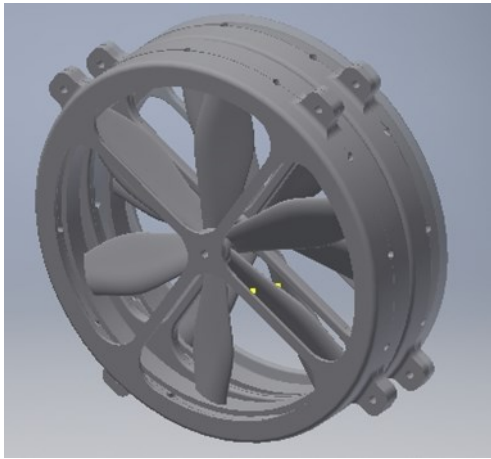

Fig. 7. CAD image of two RDF units assembled in tandem

VIII. CONCLUSION

The primary aim of this project was to investigate the feasibility of applying electrical Rim Driven Fan technology to Small Unmanned Aircraft.

As a result of the project work carried out, the conclusion reached is that RDF technology could be successfully applied to lift and propel a SUA. However, the performance testing of the RDF has demonstrated that in its current prototype form, it would not be as efficient as a conventional BLDC and propeller arrangement, such as are typically found on multi-rotor aircraft.

The project also highlighted a problematic feature of the RDF design, which relates to the cogging torque of the motor. Most BLDC motors are subject to a degree of cogging torque. However, the architecture of the RDF makes it particularly prone to high cogging torque characteristics which can affect start-up performance and cause vibration at low rotational speeds. It is therefore recommended that any future study of this technology ensures that this characteristic is addressed. In particular, it is important to ensure that the start-up torque generated on energisation of the windings is sufficient to overcome the cogging torque generated by the permanent magnetic field and stator interaction.

From the research carried out, the indications are that RDF technology has not yet been applied to any UAV applications. Furthermore, there do not appear to be any wider aerospace applications of RDF technology actually in existence. It was also concluded that any future applications of the RDF technology will most probably be found in novel UAV roles and configurations, such as:

- High speed fixed wing UAVs;
- Highly manoeuvrable vectored thrust UAVs;
- Shrouded fan vehicles including Coanda Effect UAVs;
- Amphibian UAVs;
- Miniaturised UAVs with hub-less rotors.

This project has also demonstrated that it is possible to construct a low cost RDF device which is capable of interfacing with existing commercially available UAV components such as ESCs, LiPo Batteries and Servo Regulators. Additionally, because the major bespoke parts of the concept demonstrator RDFs were made using 3D printing technology, the project has also demonstrated the possibility of being able to remotely manufacture UAV propulsion units and replacement parts. This could be a useful capability to develop for exploratory projects located in remote areas of the world or indeed on other atmospheric planets such as Mars.

REFERENCES

[1] B. Read, and T. Robinson, "The future of … UAVs," *Aerospace Magazine*, vol. 43, no. 9, pp. 14-21, Sep. 2016.

[2] Juniper Research (2015). *Drones, Consumer and Commercial Applications, Regulations and Opportunities 2015-2020* [Online]. Available: https://www.juniperresearch.com/researchstore/devices-wearables/drones/market-trends-competitive-landscape

[3] W. Thomson, *Thrust for Flight*. London: Pitman Publishing, 1972.

[4] H.E. Saunders, *Hydrodynamics in Ship Design*, vol. 2. New York: Society of Naval Architects and Marine Engineers, 1957.

[5] Voith (2016). *The Reference in Silent Thrusters: Voith Rim Drive Technology in Yachts* [Online]. Available: http://resource.voith.com/vt/publications/downloads/2152_e_vt2331_en_vit_vip_yacht_2016-05.pdf

[6] J.E. Dennis, C.A. Gallo, P.A. Solano, W.K. Thompson, and D.R. Vrnak, "Development of a 32 inch diameter levitated ducted fan conceptual design," NASA Glenn Research Centre, Cleveland, OH, Rep. NASA/TM-2006-214481, Dec. 2006.

[7] A. Hughes, *Electric Motors and Drives*, 2nd ed. Oxford: Butterworth-Heinemann Ltd., 1993.

[8] Infolytica Corporation (2016). *Electric Machine Design Software* [Online]. Available: http://www.infolytica.com/en/products/motorsolve/MotorSolve.pdf

[9] J.R. Hendershot, and T.J.E. Miller, *Design of Brushless Permanent-magnet Motors*. Hillsboro, OH: Magna Physics Pub., Oxford: Clarendon Press, 1994.

[10] J. Cox, *Electric Motors*. Poole: Special Interest Model Books Ltd., 2009.

[11] E.R. Magsino, C.M. Dollosa, S. Gavinio, G. Hermoso, N. Laco, and L.A. Roberto, "Stabilizing quadrotor altitude and attitude through speed and torque control of BLDC motors," in *Proc. 13th Int. Conf. on Control, Automation, Robotics and Vision*, Singapore, 10-12 Dec. 2014, pp. 438-443.

[12] E.A. Avallone, and T. Baumeister, *Marks' Standard Handbook for Mechanical Engineers*, 10th ed. New York: McGraw-Hill, 1996.

[13] H.I.H. Saravanamuttoo, G.F.C. Rogers, H. Cohen, and P.V. Straznicky, *Gas Turbine Theory*, 6th ed. Harlow: Pearson Education Ltd., 2009.